SAND2005-7789C

Quantification of Resolution and Noise Effects on Thermal Dissipation Measurements in Turbulent Non-premixed Jet Flames

G-H. Wang[1], R. S. Barlow[1] and N. T. Clemens[2]

[1] Combustion Research Facility

Sandia National Laboratories, Livermore, CA, 94550

[2] Department of Aerospace Engineering and Engineering Mechanics

The University of Texas at Austin, Austin, TX, 78712

Colloquium: Turbulent Flames

Keywords: Turbulent flames; Scalar dissipation; Length scale; Rayleigh scattering

Corresponding Author:

Guanghua Wang
Combustion Research Facility
Sandia National Laboratories
Livermore, CA 94551-0969

Tel: (925) 294-6535
FAX: (925) 294-2595
email: gwang@sandia.gov

Length: **5828** words (Method 1 for Word file)

Main Text:	4102
Equations:	7*(3)*7.6 = 160
References:	(31+2)*2.3*7.6 = 577
Tables:	61 + 91 = 152
Figures:	200 + 132 + 135 + 125 + 122 + 123 = 837

Quantification of Resolution and Noise Effects on Thermal Dissipation Measurements in Turbulent Non-premixed Jet Flames

G-H. Wang[1], R. S. Barlow[1] and N. T. Clemens[2]

[1] Combustion Research Facility

Sandia National Laboratories, Livermore, CA, 94550

[2] Department of Aerospace Engineering and Engineering Mechanics

The University of Texas at Austin, Austin, TX, 78712

Abstract:

One-dimensional (1-D) line Rayleigh thermometry is used to investigate the effects of spatial resolution and noise on thermal dissipation in turbulent non-premixed $CH_4/H_2/N_2$ jet flames. The high signal-to-noise ratio (SNR) and spatial resolution of the measured temperature field enables determination of the cutoff wavenumber in the 1-D temperature dissipation spectrum obtained at each flame location. The local scale inferred from this cutoff is analogous to the Batchelor scale in nonreacting flows, and at downstream locations in the flames studied here it is consistent with estimates of the Batchelor scale based on the scaling laws using local Reynolds numbers. The spectral cutoff information is used to design data analysis schemes for determining mean thermal dissipation. Laminar flame measurements are used to characterize experimental noise and correct for the noise-induced apparent dissipation in the turbulent flame results. These experimentally determined resolution and noise correction techniques are combined to give measurements of the mean thermal dissipation that are essentially fully resolved and noise-free. The prospects of using spectral results from high-resolution 1-D Rayleigh imaging measurements to design filtering schemes for Raman-based measurements of mixture fraction dissipation are also discussed.

1 Introduction

The scalar dissipation rate – defined as $\chi = 2D|\nabla\xi|^2$, where ξ is the mixture fraction and D is the molecular diffusivity – is a critical parameter in turbulent nonpremixed combustion [1,2]. Owing to its importance in combustion modeling, a great deal of recent work has been directed at the measurement of χ by using line or planar imaging of single or multiple scalars [3-9]. Scalar dissipation occurs at the finest scales of turbulence. This makes such measurements in flames particularly challenging because they require high precision and good spatial resolution. Furthermore, it is not clear how best to estimate the required resolution for a given flame condition. This is because the scaling laws that are used to estimate the dissipation length scales in non-reacting turbulent flows are not necessarily applicable in flames, where significant spatial variations in fluid properties are present and local Reynolds numbers may be quite low.

The thermal dissipation, $\chi_T = 2\alpha|\nabla T|^2$, where T is temperature and α is thermal diffusivity, does not play as fundamental a role in turbulent combustion theory. Nevertheless, it has been measured using a range of techniques [10-13]. The current study pursues the belief that the thermal dissipation measurements can help to improve the quality of scalar dissipation measurements. This is because temperature measurements from Rayleigh scattering, exhibit higher signal-to-noise ratios (SNR) than mixture fraction measurements. Therefore, thermal dissipation can be measured with higher SNR and potentially higher spatial resolution than scalar dissipation. Since the length scales of thermal and scalar dissipation structures are expected to be similar in flows with Lewis number near unity, information regarding the thermal dissipation should be directly applicable to the mixture fraction dissipation field. Furthermore, since noise and resolution effects are inherently coupled, it is anticipated that the high SNR and high

resolution of the temperature measurements will enable the decoupling of these correlated processes.

Generally, spatial averaging and noise have opposite effects, as limited resolution acts to reduce scalar gradients, whereas noise increases the measured dissipation. These opposing effects make it difficult to assess the accuracy of dissipation measurements, and most reported mixture fraction and thermal dissipation measurements have not fully quantified these effects, especially in reacting flows. The effects of spatial resolution on scalar dissipation measurements have been more thoroughly investigated in nonreacting flows [14-15], and it has been suggested [16] that it is necessary to resolve approximately one or two times the Batchelor scale, the finest scale over which turbulent fluctuations in a scalar gradient can be sustained, in order to accurately determine the mean dissipation rate.

Dissipation is proportional to the square of the gradient, so noise always acts to increase the measured dissipation. The false dissipation rate induced by noise has been termed the *apparent dissipation* [3]. Mi and Antonia [17] showed that this apparent dissipation increases without bound as the probe resolution becomes infinitely small since the noise remains finite. Similar results were found in 1-D line measurements of scalar dissipation in a non-reacting CO_2-air jet [18]. Different techniques have been used to quantify the effect of apparent dissipation in turbulent flame measurements [19]. In one approach, the magnitude of the apparent dissipation as a function of mixture fraction was quantified in a steady laminar flame [3, 20-21]. In another approach, the effect of noise on the measured scalar dissipation was studied by adding noise to large-eddy simulation data [6].

In the present study, high-resolution 1-D line Rayleigh thermometry was used to measure the energy and dissipation spectra of turbulent fluctuations in temperature in a simple

nonpremixed $CH_4/H_2/N_2$ jet flame at Reynolds numbers of 15,200 (DLR-A) and 22,800 (DLR-B). These flames have been previously studied [12, 19, 22-25] and have been used as a benchmark for the TNF Workshop [26]. The 1-D dissipation spectra are used to determine the high-wavenumber cutoff of the thermal dissipation spectrum.

This paper focuses on measurements made at downstream locations from x/d =10, 20 and 40, where the measurement resolution is demonstrated to be smaller than the cutoff in the dissipation spectrum, and noise is the primary contributor to the thermal dissipation error. It is shown that mean dissipation can be substantially in error, when determined without proper corrections or filtering to remove the effects of noise. This is similar to the conclusions drawn from the time-series measurements performed in the same flame [19] but with lower resolution and SNR than in the current study. With knowledge of the dissipation cutoff at each measurement location, digital filters combining pixel binning and differentiation are designed to suppress the noise without attenuating the true dissipation spectrum. These filtering schemes are then used to generate radial profiles of mean thermal dissipation that are essentially fully resolved and noise free.

A technique to correct for the apparent thermal dissipation induced by noise in the 1-D line measurements is also described. This involves characterizing the noise contribution in a steady laminar $CH_4/H_2/N_2$ jet flame where there are no turbulent fluctuations. Here the measured dissipation (after subtracting mean gradient) is the noise-induced apparent dissipation only, which may be represented as a function of temperature. A similar technique has been applied in mixture fraction dissipation measurements [3, 20-21], but without quantifying resolution effects. In this present work the residual noise correction is shown to be very small when proper filtering is applied to these high SNR data.

2 Experimental setup and data reduction

The experimental setup has been described previously [4-5], and only a brief overview is presented here. Four frequency-doubled Nd:YAG laser beams were combined for the Raman/Rayleigh measurements. (Raman measurements were obtained simultaneously but are not discussed in this paper.) Total energy was about 1.6 J/pulse, and the combined beam had a waist diameter of about 0.220-mm ($1/e^2$). Rayleigh scattered light was collected at right angles to the incident beam by two matched achromats (*f*/3.8) and focused onto a back-illuminated CCD detector through a 532-nm band-pass filter. The pixel-size of 0.020 mm for 1:1 imaging gives a projected pixel resolution of 0.04 mm (after on-chip binning of two pixels) along the laser beam direction. The signal was integrated across the diameter of the imaged laser beam. The resulting SNR for temperature above a premixed flat flame at ~ 2000 K was about 170.

The optical performance of the Rayleigh imaging system was analyzed using ZMAX. The measurement volume, determined by the collection optics blur effect [27] and the laser beam diameter, was 0.04 mm in length by 0.22 mm in diameter. The total imaging length along the laser beam direction was 6 mm. The probe was positioned at representative locations in the jet flames, and typically 6,000 samples were collected at each measurement location. The measured mean and *rms* temperature profiles agree well with previous Sandia point measurements [26], demonstrating repeatability of flame conditions.

The present $CH_4/H_2/N_2$ fuel mixture yields a Rayleigh cross section that is nearly independent of mixture fraction [22]. Thus temperature is determined as $T = I_{R0}T_0/I_R$, where I_{R0} is the reference Rayleigh scattering signal from air at room temperature (T_0). The radial component of thermal dissipation is $\chi_T = 2\alpha(T)(T_{,r})^2$, where comma-*r* signifies the radial

derivative. The thermal diffusivity $\alpha(T)$ representative of local conditions was calculated from $\alpha(T)=\alpha_0(T/T_0)^{1.723}$, where $\alpha_0 = 2.6\times10^{-5}(m^2/s)$ and the exponent 1.723 was determined by a curve fit to the calculated thermal diffusivity [28] with temperature and mean species concentrations from [26].

The energy and dissipation spectra for turbulent fluctuations in temperature are defined as

$$E(\kappa)=\left|\,\Im\left[T'(r)\right]\right|^2, \tag{1}$$

$$D(\kappa)=2\alpha\kappa^2E(\kappa), \tag{2}$$

where $T'(r)$ is the measured fluctuation temperature, $\Im$ is the Fourier transform operator and κ is the wavenumber. In reacting flows, thermal diffusivity is not a constant. However, if the diffusivity is replaced by its mean value at a given location in the flame, Eq. (2) can be approximated as $D(\kappa)\approx 2\langle\alpha\rangle\kappa^2E(\kappa)$. Therefore, $2\kappa^2E(\kappa)$ is used as a surrogate of the thermal dissipation spectra in the current study of spatial resolution requirements for dissipation measurements.

3 Resolution estimation from scaling laws

It is well known that in fully turbulent flows the finest spatial scales in the scalar field are of order the Batchelor scale, defined as $\lambda_B=\eta\,Sc^{-1/2}$, where $\eta=\left(\nu^3/\langle\varepsilon\rangle\right)^{1/4}$ is the Kolmogorov scale, ν the kinematic viscosity, $\langle\varepsilon\rangle$ the mean rate of kinetic energy dissipation, and $Sc=\nu/D$ the Schmidt number. However, it is not clear that laws for estimation of the smallest turbulent scales are applicable in the near field region of a jet flame because there is significant variation in local properties, local Reynolds numbers are typically low (<7000 in the present flames), and the near field is a region of developing turbulence. Nevertheless, the estimated Batchelor scale

will be a useful reference scale for comparison purposes at selected locations. Using measurements of $\langle\varepsilon\rangle$ in nonreacting round jets in [29], the Batchelor scale can be shown to be

$$\lambda_B = 2.3\delta\, Re_\delta^{-3/4}\, Sc^{-1/2}, \tag{3}$$

where $Re_\delta = U_C\delta/\nu_C$ is the local Reynolds number, with U_C the jet centerline velocity taken from [24], and δ the full width at half maximum of the velocity profile [24]. In nonreacting round jets, Re_d (jet exit Reynolds number) is approximately equal to Re_δ, but this is not true in jet flames [30]. The kinematic viscosity was calculated using [28] with mean centerline temperature and species concentrations from [26]. The estimated Batchelor scales are shown in Table 1 for the DLR-A flame at $x/d = 20$ and 40. It can be seen that the local Reynolds number at $x/d = 40$ is about a factor of five smaller than the jet exit Reynolds number (15,200). The current 1-D line system can resolve the estimated Batchelor scale at downstream locations of $x/d \geq 40$. At $x/d = 20$ in DLR-A the laser beam diameter is about $3\lambda_B$. However, because this averaging across the laser beam diameter is not along the radial gradient direction, it will result in a small error as discussed in [15]. The most important feature of the current measurement is that the temperature profiles were measured with high resolution along the laser beam (gradient) direction.

4 Results and discussions

4.1 One dimensional power spectra

Energy and dissipation spectra are shown in Fig. 1 for centerline locations (-3 mm < r < 3 mm) at x/d =10, 20 and 40 in both flames. The energy spectrum of the temperature gradient is equal to the thermal dissipation spectrum without the diffusivity, and we refer to it here as the

dissipation spectrum for brevity. The energy spectra in Fig. 1a roll off with increasing wavenumber and then go flat in the high wavenumber range. This flat part of each energy spectrum is the noise floor, and it demonstrates that the noise from different pixels along the 1-D line is uncorrelated. For the nearly constant Rayleigh scattering cross-section of the current fuel, temperature is inversely proportional to the Rayleigh signal. Therefore, the level of the noise floor follows the trend of the mean temperature, i.e. higher noise for higher temperature. We note that none of the spectra exhibit a plateau at low wavenumber because the overall length of flow imaged (6 mm) was not large enough to span a sufficient number of integral scales.

The flat noise floor in each energy spectrum gives a slope of two in the corresponding dissipation spectrum, as shown in the high wavenumber part of Fig. 1b. The valley in each dissipation spectrum is determined by competition between the true dissipation rate and noise in the measurement. It is clear that the highest wavenumber portion of these measured spectra is dominated by noise. Figure 1 shows that dissipation spectra from DLR-B are shifted to higher wavenumber (smaller length scales) relative to the corresponding spectra from DLR-A, as expected due to the increase in Reynolds number between the two cases. Figure 2 shows spectra from DLR-A at $x/d = 20$ obtained with the 6-mm probe on the centerline and at radial locations corresponding to maxima in the *rms* mixture fraction, mean temperature, and *rms* temperature. The different noise levels and spectral positions reflect the fact that properties are not uniform across the flame.

4.2 Scale estimation from spectra

Identifying the spatial scale that corresponds to the high-wavenumber cutoff in turbulent fluctuations is important in dissipation measurements, especially for laser diagnostic techniques where higher resolution will generally result in lower signal levels and SNR. It is well known in

nonreacting turbulence theory [31] that the cutoff in the kinetic-energy dissipation spectrum is at about $\kappa\eta = 1$, where κ is the wavenumber with units rad/m. Note that the physical wavelength corresponding to this cutoff is $2\pi\eta \approx 6\eta$, which indicates that scales smaller than 6η contribute little to the total mean dissipation [31]. For Schmidt and Lewis numbers near unity we have $\lambda_B \approx \eta$, and we expect the cutoff to be nearly the same for the scalar and velocity spectra at a given flow condition. The key issue for the present work is to determine the cutoff wavenumber in each measured dissipation spectrum. This was done by considering the 3-D model spectrum given by Pope [31], which shows that the cutoff ($\kappa\eta = 1$) corresponds to a power level of about 2% of the peak in the 1-D dissipation spectrum. The peak is not presented in most of the current measured 1-D spectra. Therefore, we have taken the highest value in the measured dissipation spectrum as the reference and used 1% of this value to identify the experimental cutoff κ_C. This will give a conservative estimate because the dissipation at higher wavenumbers is expected to contribute less than 1% to the total mean dissipation, based on the model spectrum. We then obtain a local scale λ_C from $\kappa_C \lambda_C = 1$ that is analogous to the Batchelor scale λ_B. Using this procedure, the estimated wavenumber for the dissipation cutoff measured on the centerline at $x/d = 40$ in DLR-A is roughly $\kappa_C = 5$ *rad/mm*, as illustrated in Fig. 3. The corresponding scale $\lambda_C = 0.2$ mm is comparable to the value $\lambda_B = 0.25$ mm estimated from scaling laws. Noted that λ_C is expected to be smaller by roughly 20-30% than the local λ_B because of the conservative procedure applied here. Also, as noted above, the physical wavelength corresponding to the cutoff is $2\pi\lambda_C$ or about 1.2 mm at this local flame condition.

For most of the measurement locations in the present study, the 1% level is reached before noise becomes important. Furthermore, because a constant noise floor (*NF)* is measured

in each energy spectrum, a noise-corrected dissipation spectrum may be obtained [19] from $2\kappa^2\left[E_m(\kappa) - NF\right]$ as illustrated in Fig. 3, so that the 1% level may be determined at all locations. Table 2 lists values of λ_C for all of the measurement locations considered. At a given spatial location λ_C is smaller in DLR-B (Re_d = 22,800) than in DLR-A (Re_d = 15,200), as expected. However, the ratio, $(\lambda_C)_{DLR-B}/(\lambda_C)_{DLR-A}$, is about 0.82 on average, while Eq. (3) would predict a ratio of 0.74 for nonreacting jets. The reasons for this are not clear at present. The experimentally determined cutoff scale generally increases with downstream distance in each flame — also expected. At streamwise locations x/d = 10 and 20, λ_C is smallest on the centerline, due to the lower temperature, and increases with radial distance. At x/d = 40 the scale is nearly constant across each flame. This behavior is qualitatively consistent with observations in [5] regarding the length scale associated with turbulent fluctuations of the mixture fraction in piloted jet flames.

Comparison of corresponding values of λ_C and λ_B (Table 1) suggests that the scaling law from nonreacting flow (Eq. 3) can provide a reasonable estimate of the smallest turbulent scales in the downstream portion of a simple jet flame ($x/d \geq 20$). However, caution should be used in applying such scaling laws closer to the nozzle, where there can be significant radial variation in fluid properties and local turbulence scales. Furthermore, direct measurement of the scalar spectrum, as applied here, will be the most effective approach to determining resolution requirements and local turbulence scales in complex flames, such as bluff-body or swirl-stabilized flames. We also note that scale information, as in Table 2, may be useful for design or evaluation of grids for large-eddy simulation (LES).

4.3 Noise reduction by digital filtering

With knowledge of the experimentally determined cutoff κ_C for the dissipation spectrum at each measurement location, the next step is to identify appropriate digital filtering schemes to suppress noise without attenuating the dissipation spectrum at wavenumbers lower than κ_C. This is possible only when the dissipation spectrum is measured without significant noise effects and the experiment is over-resolved. Both are true in the current study.

The calculated gradient can be more generally expressed as the result of a filtering process, $T_{,r} = h_g * T$, where h_g is a digital filter for gradient calculation and * is the convolution operator. If a smoothing (e.g. pixel-binning) filter h_p is applied, the measured gradient is then calculated as,

$$\left(T_{,r}\right)_m = h_p * h_g * T + h_p * h_g * n \tag{4}$$

where n is the noise. The design objective is to keep the filtered gradient $h_p * T_{,r}$ close to the true $T_{,r}$, while minimizing the filtered noise gradient $h_p * n_{,r}$ ($n_{,r} = h_g * n$). In the current study, pixel-binning and two common difference stencils are utilized as examples of the large family of possible filters.

Figure 3 illustrates the dissipation spectra calculated using ideal differentiation in Eq. (2) (without diffusivity), first order one-side difference (H12B), and second order central difference (H22C). As mentioned above, the flat noise floor in the energy spectrum gives a slope of two in the dissipation spectrum from Eq. (2). The H12B filter behaves similarly until close to the half sampling wavenumber. If left unfiltered, the integrated area under this noise portion of the spectrum (in linear coordinates) would be a major contributor to the measured dissipation. When the measurement is over-resolved, the H22C stencil can reduce the noise significantly as

compared to H12B. Figure 3 also shows the effect of pixel-binning in combination with the central difference scheme. The digital filter shape is determined by the specific stencil, but this shape is shifted to lower wavenumbers after pixel-binning. Therefore, the difference stencil and binned-pixel resolution combine together to determine their net effect on the true dissipation and noise spectra. Using the central difference scheme, the $x/d = 40$ data can be binned by 2 or 4 without affecting the true dissipation spectra. Figure 3 shows that the noise is significantly attenuated when the central differencing scheme is applied with 4-pixel binning. For both flames full resolution can be maintained with binning the pixels by 4 at $x/d = 40$, 2 at $x/d = 20$, and no-binning at $x/d = 10$. However, for under-resolved experiments, the true dissipation spectra will be attenuated by the central difference stencil, and the resolution effect on the measured dissipation rate will have to be considered.

4.4 Noise correction to mean dissipation

The noise-induced apparent dissipation and techniques to correct for it have been discussed in the context of scalar dissipation measurements in nonreacting [17] and reacting [19-20] flows. Apparent dissipation is defined as

$$\chi_a \equiv \left\langle \left(\chi_T\right)_m \right\rangle - \left\langle \chi_T \right\rangle, \tag{5}$$

where the subscript *m* indicates the noise affected measurement and $\left\langle \chi_T \right\rangle$ is the true mean value. For a uniform flow or laminar flame it may be shown [19] that the apparent dissipation due to noise can be expressed as $\chi_a = 2\left\langle \alpha_m \left(n_{,r}\right)^2 \right\rangle$. For the current measurements the noise induced variance of thermal diffusivity is very small, and the apparent thermal dissipation comes primarily from the noise contribution to the measured temperature gradient.

The apparent dissipation may be determined from measurements in a steady laminar jet flame of the same fuel mixture by subtracting the true laminar dissipation (based on mean profiles) from the total and expressing the result as a function of temperature. The true mean thermal dissipation rate in the turbulent flames may then be determined on a conditional basis as,

$$\langle \chi_T \,|\, T \rangle_{turb} = \langle (\chi_T \,|\, T)_m \rangle_{turb} - \langle (\chi_a \,|\, T)_m \rangle_{lam} . \tag{6}$$

The apparent dissipation depends on the processing scheme (pixel binning and differencing), so this correction procedure requires that the same scheme be applied to both laminar and turbulent data.

Figure 4 compares the apparent dissipation from the laminar flame calculated using two differencing schemes and two levels of pixel binning. The apparent dissipation is much higher for the H12B than for the H22C, which is consistent with results shown in Fig. 3, where the H22C scheme attenuates the noise contribution significantly compared to H12B. This demonstrates that the measured dissipation depends on the difference stencil, as well as noise and resolution effects, and all these must be considered when comparing different experimental results or comparing experiments with numerical simulations. Note also that the apparent dissipation scales approximately as T^5, which is a result that was predicted in the shot-noise limited analysis developed in [19].

To obtain radial profiles of the corrected mean thermal dissipation in the turbulent flame the procedure is to first calculate the corrected conditional average of the thermal dissipation rate at each location from Eq. (6) and then calculate the corrected mean thermal dissipation as

$$\langle \chi_T \rangle_{turb} = \int \langle \chi_T \,|\, T \rangle_{turb} P(T) dT . \tag{7}$$

where $P(T)$ is the PDF of the temperature at the measurement location.

4.5 Mean thermal dissipation profiles

Figure 5 compares radial profiles of uncorrected and corrected mean thermal dissipation rate for the four radial positions at $x/d = 40$ in flame DLR-A. Results for two different digital filtering schemes are included in order to illustrate the potential importance of noise in dissipation measurements as well as the effectiveness of the present filtering and correction schemes for reducing noise-induced errors. The two sets of results both use the H22C differencing but with different levels of pixel binning. As expected from the dissipation spectra in Fig. 3, the central differencing stencil combined with the proper level of pixel binning works as a digital filter to reduce noise induced apparent dissipation significantly, such that there is very little difference between the uncorrected and corrected profiles. Therefore, the properly filtered and corrected thermal dissipation results from the current experimental system are fully resolved at these flame locations and essentially free of noise effects. The result for $N_{Bin} = 1$ demonstrates that the noise contribution to the mean thermal dissipation rate can be significant when the measurements are over resolved. Even though the measured mean dissipation with $N_{Bin} = 1$ includes a significant contribution from noise, the correction procedure still yields nearly the same corrected profiles as for $N_{Bin} = 4$, the binning scheme selected to minimize noise without attenuating the true dissipation spectrum. This implies that the correction based on the laminar flame technique is reasonably robust when applied to the present turbulent flame. In order to reduce the uncertainty of the corrected mean radial dissipation profiles, the subtracted or apparent dissipation should be kept as small as possible by proper filter design.

Radial profiles of the filtered and corrected thermal dissipation from all measurement locations in both flames are shown in Fig. 6. At each streamwise location the profile shapes in DLR-A and DLR-B are very similar. Thermal dissipation levels are consistently higher in DLR-

B, but by a smaller ratio than one might expect, based of the 1.5 ratio of jet Reynolds numbers. This is due, at least in part, to the fact that the contribution to the total dissipation from the mean temperature gradient is not trivial in these flames, especially at $x/d = 10$, and this mean contribution does not increase with Reynolds number.

As discussed in the section 4.3, the combination of pixel binning and the H22C scheme represents only a convenient example of many possible digital filters that might be used to reduce noise in dissipation measurements. Special digital filters can reduce noise even more effectively, and further work is being done to test such filters on the present data sets. Furthermore, if the mixture fraction dissipation follows the same roll-off behavior at the high wavenumber end of the spectrum (as may be expected for $Le \sim 1$), these designed digital filters based on the fully resolved thermal dissipation spectra can be applied to the corresponding mixture fraction dissipation measurements, which generally exhibit higher noise levels and reduced spatial resolution. In this context it is important to emphasize that the effective resolution of any gradient and dissipation measurements depends on both the physical (optical) resolution and the processing schemes that are applied.

5 Conclusions

High-resolution 1-D line Rayleigh thermometry was used to measure spectra of temperature fluctuations and the thermal dissipation rate in turbulent non-premixed $CH_4/H_2/N_2$ jet flames. The spatial resolution and signal-to-noise ratio of the current experiment enabled the study of the correlated effects of resolution and noise. The 1-D power spectra of the temperature fluctuations were used to determine the cutoff of the dissipation spectrum and the corresponding spatial scale. The local scale inferred from this cutoff is analogous to the Batchelor scale in nonreacting flows, and at downstream locations in the flames studied here it is consistent with estimates of the

Batchelor scale based on the scaling laws using local Reynolds numbers. Knowledge of the cutoff wavenumber allowed the design of digital filtering schemes for calculating thermal gradients that significantly reduced noise without attenuating the true dissipation spectrum. A procedure to correct for the apparent dissipation due to noise was applied based on measurements of the apparent dissipation in a laminar $CH_4/H_2/N_2$ jet flame. These experimentally determined spectral cutoff and noise correction techniques combined together give measurements of the mean thermal dissipation that are essentially fully resolved and noise-free. The procedure described will be useful in line Raman/Rayleigh/LIF experiments where both temperature and mixture fraction are measured, as it will enable a more accurate *in situ* determination of the local resolution requirements for mean scalar dissipation.

Acknowledgment

This work was supported by the Division of Chemical Sciences, Geosciences and Biosciences, Office of Basic Energy Sciences, US Department of Energy. Sandia National Laboratories is a multiprogram laboratory operated by Sandia Corporation, a Lockheed Martin Company, for the United States Department of Energy under contract DE-AC04-94-AL85000. Technical support of R. Harmon and M. Boisselle during the experiments is gratefully acknowledged.

References

1. R.W. Bilger, *Combust. Sci. Tech.* 13 (1976) 155-170.
2. N. Peters, *Turbulent Combustion*, New York: Cambridge University Press, 2000.
3. S.P. Nandula, T.M. Brown, R.W. Pitz, *Combust. Flame*. 99 (1994) 775-783.
4. A.N. Karpetis, R.S. Barlow, *Proc. Combust. Inst.* 29 (2002) 1929-1936.
5. R.S. Barlow, A.N. Karpetis, *Proc. Combust. Inst.* 30 (2005) 673-680.
6. D. Geyer, A. Kempf, A. Dreizler, J. Janicka, *Proc. Comb. Inst.* 30 (2005) 681-689.
7. S.H. Stårner, R.W. Bilger, M.B. Long, J.H. Frank, D.F. Marran, *Combust. Sci. Tech.* 129 (1997) 141-163.
8. J.H. Frank, S.A. Kaiser, M.B. Long, *Proc. Combust. Inst.* 29 (2002) 2687-2694.
9. J.A. Sutton, J.F. Driscoll, *Proc. Combust. Inst.* 29 (2002) 2727-2734.
10. L. Boyer, M. Queiroz, *Combust. Sci. Tech.* 79 (1991) 1-34.
11. E. Effelsberg, N. Peters, *Proc. Combust. Inst.* 22 (1988) 693-700.
12. G-H. Wang, N.T. Clemens, P.L. Varghese, *Proc. Comb. Inst.* 30 (2005) 691-699.
13. D.A. Everest, J.F. Driscoll, W.J.A. Dahm, D.A. Feikema, *Combust. Flame* 101 (1995) 58-68.
14. J.C. Wyngaard, *Phys. Fluids* 14 (1971) 2052-2054.
15. R.A. Antonia, J. Mi, *Exp. Fluids* 14 (1993) 203-208.
16. J. Mi, G.J. Nathan, *Exp. Fluids* 34 (2003) 687-696.
17. J. Mi, R.A. Antonia, *Exp. Thermal Fluid Sci.* 8 (1994) 328-335.
18. P. Ferrão, M.V. Heitor, R. Salles, 10th International Symposium on Turbulence, Heat and Mass Transfer, Lisbon, Portugal, (2000) p. 12.7.
19. G-H. Wang, N.T. Clemens, P.L. Varghese, *App. Optics* 44 (2005) 6741-6751.

20. D. Geyer, *1D-Raman/Rayleigh experiments in turbulent-opposed jet flows*. PhD thesis, Technische Universit¨at Darmstadt, (2004).

21. J.H. Frank, S.A. Kaiser, M.B. Long, *Comb. Flame* 143 (2005) 507-523.

22. V. Bergmann, W. Meier, D. Wolff, W. Stricker, *Appl. Phys. B* 66 (1998) 489-502.

23. W. Meier, R.S. Barlow, Y-L. Chen, J-Y. Chen, *Combust. Flame* 123 (2000) 326-343.

24. Ch. Schneider, A. Dreizler, J. Janicka, E.P. Hassel, *Combust. Flame* 135 (2003) 185-190.

25. M.W. Renfro, J.P. Gore, N.M. Laurendeau, *Comb. Flame* 129 (2002) 120-135.

26. International Workshop on Measurement and Computation of Turbulent Nonpremixed Flames (TNF), http://www.ca.sandia.gov/TNF/

27. N.T. Clemens, "Flow Imaging", In *Encyclopedia of Imaging Science and Technology*, John Wiley and Sons, New York, (2002) 390-419.

28. Software Tools, http://navier.engr.colostate.edu/tools/

29. C. Friehe, C.W. Van Atta, C.H. Gibson, Turbulent Shear Flows (AGARD) CP-93 (1971), p. 18-1 to 18-7.

30. L. Muniz, M.G. Mungal, *Combust. Flame* 126 (2001) 1402-1420.

31. S.B. Pope, *Turbulent Flows*, Cambridge University Press, New York, 2000.

Tables

Table 1
Estimates of resolution requirements from Eq. (3).

x/d	T [26]	ν_C [28]	U_C [24]	δ/d [24]	Re_δ	λ_B
	K	cm^2/s	m/s			μm
20	905	1.07	33.9	2.60	6580	70
40	1576	2.66	18.3	5.19	2850	250

Table 2
Experimentally determined scale λ_C [μm]. Radial positions in mm are shown in parentheses.

Case	x/d	r_1=0	r_2	r_3	r_4
A	10	53	83 (8)	106 (12)	
	20	94	120 (11)	123 (16)	145 (21)
	40	195	179 (13)	188 (29)	191 (35)
B	10	41	67 (8)	84 (12)	
	20	73	94 (11)	105 (16)	125 (21)
	40	163	157 (13)	159 (29)	165 (35)

Figure captions

Fig. 1. Energy and dissipation spectra of fluctuating temperature T' in DLR-A (bold lines) and DLR-B (thin lines).

Fig. 2. Energy and dissipation spectra of fluctuating temperature T' at four radial locations in DLR-A at $x/d = 20$.

Fig. 3. Dissipation spectra of fluctuating temperature T' at $x/d = 40$ in DLR-A calculated by using different stencils and by applying noise floor correction.

Fig. 4. Apparent dissipation from the laminar flame measurement using different combinations binning and differencing filters.

Fig. 5. Measured and corrected profiles of mean thermal dissipation at $x/d = 40$ in DLR-A.

Fig. 6. Corrected profiles of mean thermal dissipation in DLR-A (bold lines) and DLR-B (thin lines).

Figures

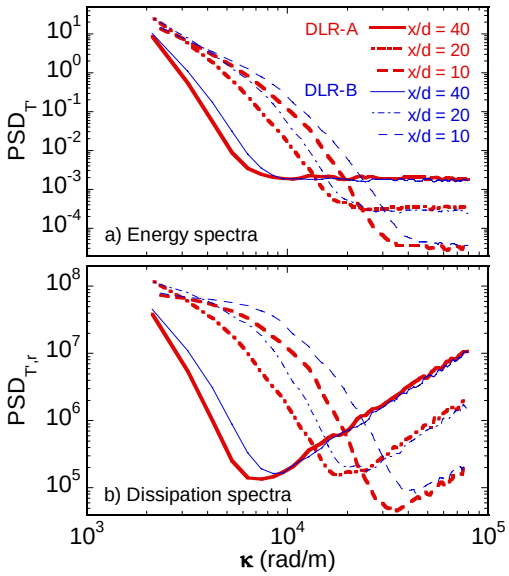

Fig. 1. Energy and dissipation spectra of fluctuating temperature T' in DLR-A (bold lines) and DLR-B (thin lines).

[color figure in electronic versions only]

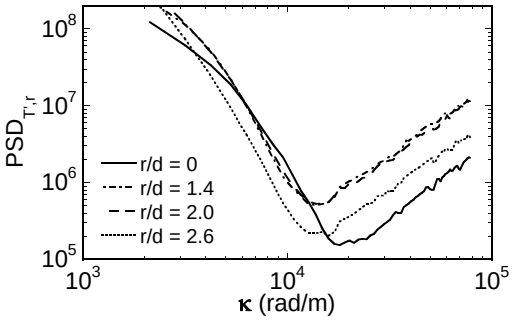

Fig.2. Energy and dissipation spectra of fluctuating temperature T' at four radial locations in DLR-A at $x/d = 20$.

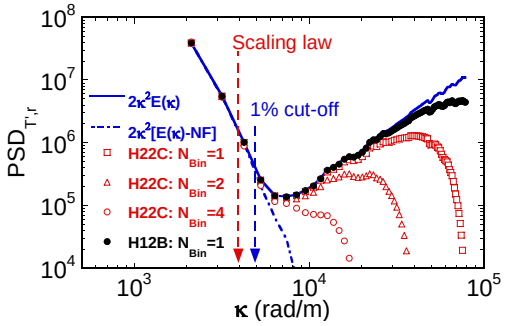

Fig. 3. Dissipation spectra of fluctuating temperature T' at $x/d = 40$ in DLR-A calculated by using different stencils and by applying noise floor correction.

[color figure in electronic versions only]

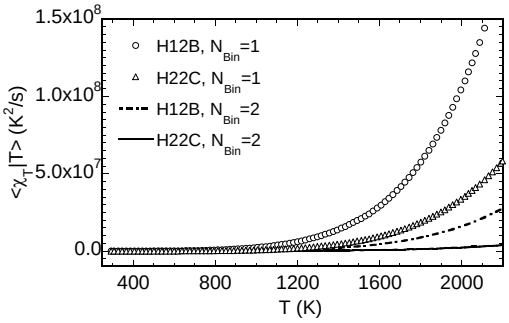

Fig. 4. Apparent dissipation from the laminar flame measurement using different combinations binning and differencing filters.

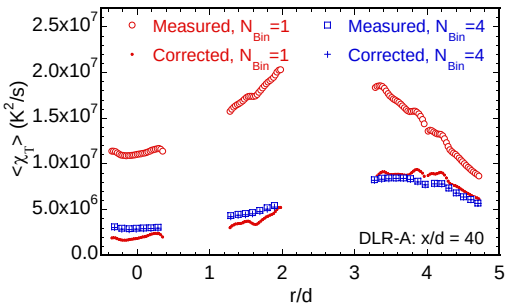

Fig. 5. Measured and corrected profiles of mean thermal dissipation at $x/d = 40$ in DLR-A.

[color figure in electronic versions only]

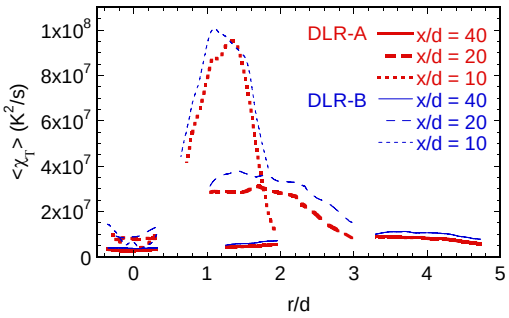

Fig. 6. Corrected profiles of mean thermal dissipation in DLR-A (bold lines) and DLR-B (thin lines).

[color figure in electronic versions only]